Evolution of mantle structure beneath the northwest Pacific: Evidence from seismic tomography and paleogeographic reconstructions

Meghan S. Miller [1] and Brian L. N. Kennett[1]

Received 28 September 2005; revised 16 January 2006; accepted 27 March 2006; published 1 July 2006.

[1] Plate motions and subducting slab morphology are intricately connected, and through the integration of seismicity, tomographic images, and relative plate motions, the evolution of mantle structure can be interpreted. Tomographic images of *P* wave, shear wave speed, and bulk sound speed perturbations of the northwest Pacific region have been interpreted to define the extent and geometry of the subducting Pacific plate. We have found that the subducted Pacific plate beneath the Japan and Kurile arcs is coherent but is very complex at the junction of the two arcs near the Hokkaido corner, as the slab subduction angle decreases from north to south while the slab thickens. The Pacific slab beneath the Japan arc is slightly thinner and subducting through the upper mantle at a less steep angle than the slab beneath the Kurile arc. As the slab reaches the 660-km discontinuity it becomes stagnant and lies in a horizontal position on top of the transition zone both beneath the Izu and Japan arcs. In contrast, the slab beneath the Kurile arc is subducting at a steeper angle and penetrates through the transition zone into the lower mantle. The difference in slab morphology appears to be due to a combination of change in dip of the subducting plate and the convergence velocity of the Pacific plate along the margin. A new paleogeographic reconstruction of northeast Asia was assembled to evaluate the plate motions that could explain the foundation of the current slab morphology. The plate reconstruction was based on Euler pole motions of the Pacific, Philippine, Amurian, Okhotsk, and North American plates relative to stable Eurasia plate. The new tectonic model illustrates the collision of the Japan and Kurile arcs, the opening of the Kurile Basin, disparity in Pacific plate velocities along the arc, and different rates of trench retreat along the Izu, Japan, and Kurile segments of the western Pacific margin. The plate motion model was interpreted in conjunction with the physical properties of the mantle imaged with the *P* wave and joint tomography to assess the evolution of the Pacific plate morphology since the mid-Miocene and to provide constraints on the plausible plate motions in the region. **Citation:** Miller, M. S., and B. L. N. Kennett (2006), Evolution of mantle structure beneath the northwest Pacific: Evidence from seismic tomography and paleogeographic reconstructions, *Tectonics*, *25*, TC4002, doi:10.1029/2005TC001909.

1. Introduction

[2] The plate motions in the northwest Pacific are complex, but the history and magnitude of velocities have been determined with GPS measurements and focal mechanisms and then extrapolated with plate tectonic reconstructions. The Pacific plate is currently converging at a rate of ~8.2–9.2 cm/yr to the northwest beneath the Kurile and Japan arcs but more slowly (~6 cm/yr) beneath the Izu arc [*Seno et al.*, 1993; *DeMets et al.*, 1994]. The Philippine Sea plate is subducting northward beneath Japan, and the Okhotsk and Amurian plates are moving slowly northeastward [*Wei and Seno*, 1998; *Zang et al.*, 2002] (Figure 1). The northwest Pacific is composed of the Eurasian, Philippine, Amurian, Okhotsk, and North American plates, yet many previous reconstruction models in the literature focus solely on the Philippine Sea plate motion or the tectonic history of Japan based on geologic data and plate motions defined by Euler poles [*Seno and Maruyama*, 1984; *Otofuji et al.*, 1985a; *Otofuji and Matsuda*, 1987; *Otsuki*, 1990; *Seno et al.*, 1993; *Fournier et al.*, 1994; *Jolivet et al.*, 1994; *Hall et al.*, 1995a]. The limited scale of these models do not take into account the motions of the other plates and arcs (or trenches) along the western Pacific margin. In addition to GPS and geologic data tomographic images can be valuable in describing the possible plate motions during the Cenozoic. The structure of the mantle interpreted from the tomograms can be explained as a result of the change in plate boundary configurations. Therefore integration of the interpreted slab morphology with a new paleogeographic tectonic reconstruction of the five plate system describes the four-dimensional tectonic evolution of the northwest Pacific during the Cenozoic.

2. Previous Models

2.1. Seismicity and Tomography Models

[3] Previously, structural features in the mantle of the northwest Pacific have been defined by models integrating seismicity and seismic tomography data [*Burbach and*

[1]Research School of Earth Sciences, Australian National University, Canberra, ACT, Australia.

0278-7407/06/2005TC001909

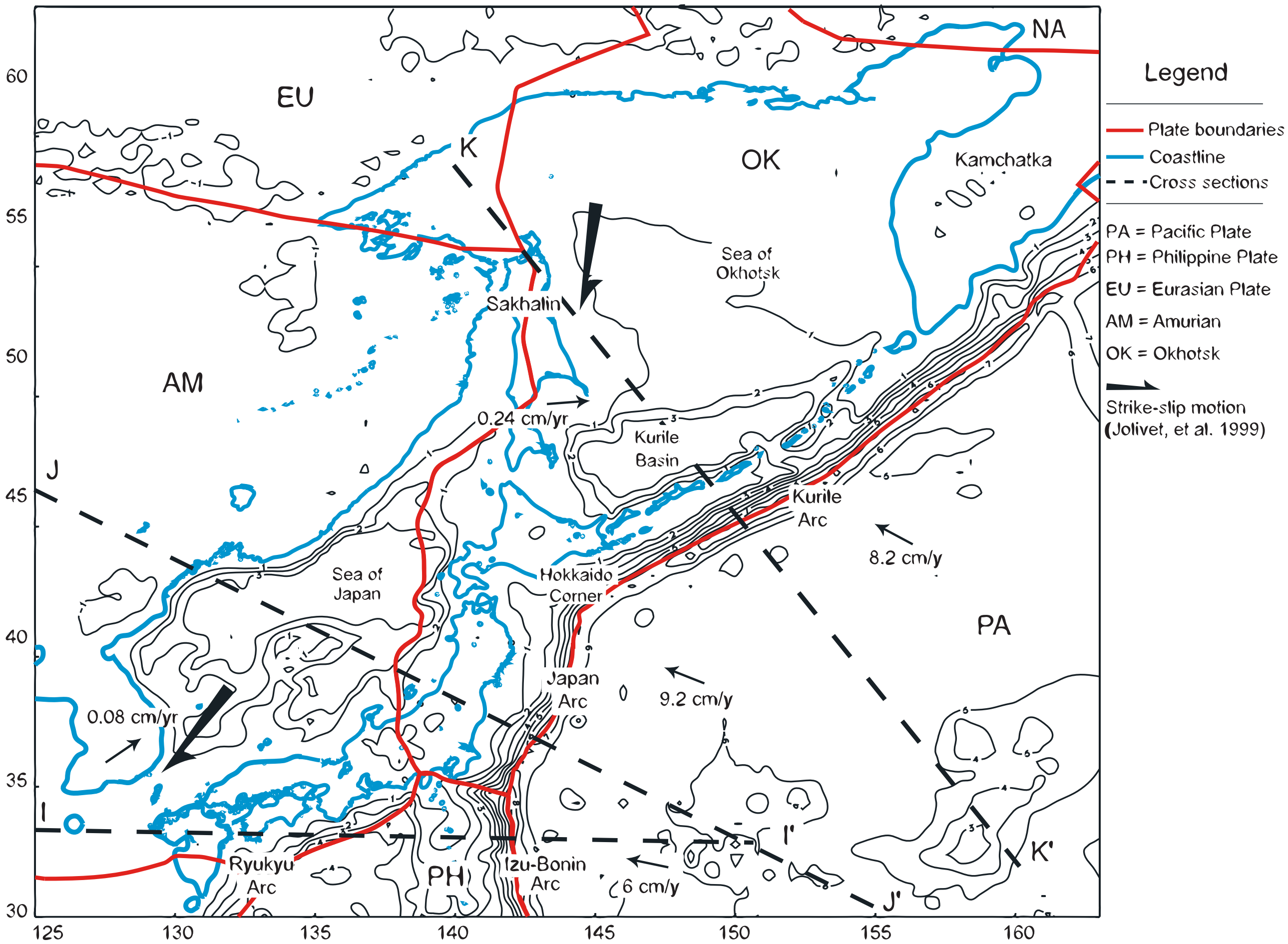

Figure 1. Map of the northwest Pacific region with plate boundaries of the Eurasian (EU), Pacific (PA), Philippine Sea (PH), Amurian (AM), Okhotsk (OK), and North American (NA) plates defined by *Bird* [2003], plate velocities [*Seno et al.*, 1993; *DeMets et al.*, 1994; *Zang et al.*, 2002], ETOPO5 bathymetry contoured in 1 km increments, and location of the cross sections in Figure 3. Large arrows show simplified zones of deformation from *Jolivet et al.* [1994].

Frohlich, 1986; *Zhou et al.*, 1990; *Chiu et al.*, 1991; *van der Hilst et al.*, 1991; *Fukao et al.*, 1992; *Zhao et al.*, 1992b; *van der Hilst et al.*, 1993; *Zhao and Hasegawa*, 1993; *Miyamachi et al.*, 1994; *Gudmundsson and Sambridge*, 1998; *Moriya et al.*, 1998]. Some researchers have investigated the morphology of the subducting Pacific plate by combining different modeling techniques [*van der Hilst and Seno*, 1993], but few have considered the complete western Pacific region from Kamchatka south to the Izu-Bonin arc [*Miller et al.*, 2006b]. Even fewer studies have integrated complementary data sources to unravel the complex nature of multiple plate boundaries, differing characteristics of subduction zones, and the large extent of the Pacific plate which make modeling the region a challenge.

[4] Models by *Chiu et al.* [1991] and *Gudmundsson and Sambridge* [1998] defined the morphology of the subducting lithosphere in the western Pacific using seismicity instead of tomographic images. *Chiu et al.* [1991] modeled the configuration of the subducted lithosphere with a surface that approximately matches the spatial distribution of earthquakes along the upper plate boundary. They noted that the deeper portions of the modeled slabs have a more complex morphology, which may be related to motion between the shallow slab and the material at depth. *Gudmundsson and Sambridge* [1998] also created a three-dimensional model of subducting slabs in the western Pacific by contouring slab-related seismicity to define the top of the slab and assuming a constant 200 km thick oceanic lithosphere. The morphology is simplified since the slab extent is based on earthquakes and a projection of constant thickness, yet it describes slab complexity and general characteristics of the geometry along the entire western Pacific margin. Their model depicts the associated changes in dip and thickness along the plate boundary as a smooth, continuous curved shape. Both the *Gudmundsson and Sambridge* [1998] and *Chiu et al.* [1991] models span the entire Pacific plate boundary, unlike other models, but the geometry is dependent on earthquake hypocenters, constant thickness for the slab, and have not been verified using the tectonic history of the region.

Table 1. Total Rotation Vectors Used in Paleogeographic Reconstruction[a]

Plate Pair	Begin, Ma	End, Ma	Latitude, °N	Longitude, °E	Rotation Angle, deg	References
EU-PA	0	10	62.33	−85.03	9.4	*Wei and Seno* [1998]
EU-PA	0	20	68	283	14.7	*Engebretson et al.* [1985]
EU-PH	0	3	50.55	158.67	3.54	*Wei and Seno* [1998]
EU-PH	0	8	48.23	156.97	8.68	*Seno et al.* [1993]
EU-PH	0	25	15	160	27.25	*Hall et al.* [1995a, 1995b]
EU-NA	0	10.6	63.61	134.05	−2.45	*Wei and Seno* [1998]
EU-NA	0	19.7	68.92	136.74	−4.97	*Lawver et al.* [1990]
EU-OK	0	20	−52.73	−37.22	9.04	*Wei and Seno* [1998]
EU-AM	0	20	60.42	123.3	0.5	*Wei and Seno* [1998]

[a]For motion of the second-listed plate with respect to the first-listed plate with positive rotations anticlockwise when viewed from above the surface of the Earth. EU, Eurasian plate; PA, Pacific plate; PH, Philippines Sea plate; NA, North American plate; OK, Okhotsk plate; and AM, Amurian plate.

[5] Other early investigations of the mantle structure using seismic tomography were limited by low-resolution images and assumptions made to simplify the modeling process making smaller-scale structures more difficult to resolve. Many of the models were primarily regional studies of the mantle or crust beneath Japan, the Philippine Sea, or Kamchatka [*Zhao et al.*, 1992a; *van der Hilst et al.*, 1993; *Zhao and Hasegawa*, 1993; *Zhao et al.*, 1994; *Gorbatov et al.*, 1999]. For example, *van der Hilst et al.* [1993] imaged the mantle beneath western Pacific island arcs using *P* and *pP* data. These images depicted zones of continuous high-velocity below the deepest earthquakes below the Kurile arc into the lower mantle and a deflected slab in the transition zone beneath Japan. The imaged dip of the slab decreased southward along strike of the Kurile-Japan arc and then widened dramatically at depth into a subhorizontal position. Beneath these arcs the *P* wave velocities were imaged in the lower mantle, but were ambiguous due to poor vertical resolution and limitations in the data and methodology.

[6] As technology and data quality improved more recent studies have been able to define the geometry of the whole western Pacific and in specific regions with more detail using enhanced methodology and larger data sets [*Widiyantoro*, 1997; *Widiyantoro et al.*, 1999; *Gorbatov et al.*, 2000; *Gorbatov and Kennett*, 2003]. The use of a combination of *P* wave, bulk sound, and shear wave speed inversions have provided more detail about the change in physical properties and structure within the mantle along the northwest Pacific [*Kennett et al.*, 1998; *Gorbatov and Kennett*, 2003; *Kennett and Gorbatov*, 2004; *Miller et al.*, 2005]. Interpretations about the age, rigidity, viscosity, and strength of the subducting oceanic lithosphere can be made using a combination of high-resolution tomographic images.

2.2. Paleogeographic Reconstruction Models

[7] There are a few proposed models that explain the tectonic evolution of the Japan arc and its surrounds. One group of researchers have based their model on paleomagnetic data and infer that the opening of the Sea of Japan and the curvature of the Japanese Island arc system has been formed as northeast Japan has rotated anticlockwise ∼47° and southwest Japan has rotated clockwise 56° since the early Miocene [*Otofuji and Matsuda*, 1983; *Otofuji et al.*, 1985b; *Otofuji and Matsuda*, 1987]. They suggested that the fan-shaped opening of the Sea of Japan was a phenomenon of rifting of a continental fragment from thick continental lithosphere. These paleomagnetic results have then been interpolated and improved upon to yield reconstructions of northeast Asia and Japan in particular.

[8] Alternative reconstructions describe the opening of the Sea of Japan and evolution of the northwest Pacific in terms of deformation of the entire Asian continent, transpressional regimes in the back arc, migration of the volcanic front, and changes to the current state of compression [*Jolivet et al.*, 1989; *Fournier et al.*, 1994; *Jolivet et al.*, 1994, 1999]. Instead of the rigid “swinging door” motion proposed for the opening of the Sea of Japan based on paleomagnetic data, evidence from Ocean Drilling Project (ODP) legs 127 and 128 suggest that dextral motion along large strike-slip faults have controlled the East Asian marginal basins and the current tectonic configuration [*Jolivet and Tamaki*, 1992; *Jolivet et al.*, 1994]. It has been proposed that two primary shear zones controlled the opening of the Sea of Japan with the N-S striking Tym-Poronaysk fault (and other parallel faults) in Sakhalin and a wide shear zone along the continental margin in the southwest near Korea (Figure 1). The dextral motion along the shear zone running from Sakhalin to northeastern Hokkaido has been found to be consistent since the early to middle Miocene and is still currently observed in geodetic and field data, as well as with focal mechanisms [*Fournier et al.*, 1994]. This transpressional regime established in the Miocene could have caused a clockwise rotation in the back arc and counterclockwise rotation in the north. The larger dextral slip in the east than the west may have been accommodated by rotation of southwest Japan and evolution into the current arcuate shape of Japan [*Jolivet et al.*, 1991; *Jolivet and Tamaki*, 1992; *Jolivet et al.*, 1994]. This reconstruction is based on evidence of motion in the shear zones and the migration of the volcanic front over the past 30 Myr. The estimated migration of the active volcanic belt was based on a simple concept that assumes that the slab dip has remained constant since the mid-Oligocene.

[9] Other plate motion studies have focused on the determination of the plate geometry in the northwest Pacific. The motion of the Okhotsk and Amurian plates have been hard to distinguish from the North American and Pacific plate motion, and only recently have the location of these bound-

aries established. Earthquake slip vectors along Sakhalin Island and the eastern margin of the Sea of Japan were used to determine the motions and boundaries of the Okhotsk and Amurian plates [*Seno et al.*, 1996; *Wei and Seno*, 1998; *Bird*, 2003]. As the motions are consistent with recent tectonics and best fitting Euler vectors (Table 1), they must be considered when reconstructing the paleogeography and tectonic history of the region although the rates are slow.

3. Seismic Tomography

3.1. Tomographic Controls

[10] The models presented in this study are based on regional body wave joint tomographic inversion of *Gorbatov and Kennett* [2003] together with a *P* wave tomographic inversion were produced from the same arrival time data [*Miller et al.*, 2005]. The detailed joint inversion data sets used an inversion algorithm introduced by *Kennett et al.* [1998] and then adapted by *Gorbatov and Kennett* [2003] to include 3D ray tracing. In this method the trajectory of seismic ray propagation between source and receiver through the three-dimensional structure of the earth is included, which improves the resolution of gradients and strong variations in wave speeds. The joint inversion used *P* and *S* arrival time data with the same source and receiver from the global catalogue of *Engdahl et al.* [1998]. Single rays with both *P* and *S* readings were picked for events and stations within the study area to optimize data coverage and to ensure that the final images could be directly compared. Mantle structure in the surrounding western Pacific was parameterized into a nonoverlapping grid of $5^\circ \times 5^\circ$ with 16 layers ranging from 35 to 200 km down to a total depth of 1600 km. The study area consisted of a grid of 19 layers with cells $0.5^\circ \times 0.5^\circ$ in the uppermost mantle, $1^\circ \times 1^\circ$ in the transition zone and lower mantle, and $2^\circ \times 2^\circ$ beneath continents to a depth of 1500 km. The final data set contained 900,000 pairs of *P* and *S* ray paths used the ak135 model as reference [*Kennett et al.*, 1995]. This nested iterative approach resulted in *P* and *S* models that were then used in a nonlinear joint tomographic inversion for bulk sound and shear wave speed inversions [*Gorbatov and Kennett*, 2003]. Then a separate *P* wave tomographic inversion was obtained with a similar nonlinear scheme using the same data set as in the joint tomography and with the same inversion parameters, but using a standard tomographic formulation [*Miller et al.*, 2005]. Although the inversion schemes used for joint tomography and the *P* wave tomography are different, the three inversions can be compared with careful consideration of the smoothing (damping) parameters. We present the *P* wave, shear wave speed, and bulk sound images to illustrate the structure of the subducting Pacific plate beneath the junction of the Japan and Kurile arcs using earthVision™ software.

3.2. Tomographic Images

[11] The tomographic images presented are a subset of the full models from *Gorbatov and Kennett* [2003] and *Miller et al.* [2005] with a maximum depth of 850 km and range between 130°–150°E and 31°–51°N (Figure 2). The large number of seismic stations and earthquake events in the area, the recorded teleseismic events, and small cell size allow for the structure of the subducting slab to be well resolved. A convenient way to measure the data coverage is the sum of the lengths of the ray segments traversing each cell. This is illustrated in Figure 3 of *Miller et al.* [2006a] with ray density plots, which show very consistent high ray density across the regions where subduction zone features are expected beneath the Japan and Kurile arcs. Detailed resolution tests using a synthetic model, from *Gorbatov and Kennett* [2003], concluded the image of the subducted slab could be recovered along its complete extension using the same inversion parameters as in the observed data. Fast wave speed anomalies used to define the subducting slab in the *P* wave inversion and shear wave speed are clearly imaged down to at depth of least 800 km (Figures 2 and 3).

[12] The interpreted dip of the Pacific plate is imaged as decreasing from north to south along the northwest Pacific convergent margin, consistent with previous studies [*van der Hilst et al.*, 1991; *van der Hilst and Seno*, 1993; *van der Hilst et al.*, 1993; *Miyamachi et al.*, 1994; *Widiyantoro et al.*, 2000; *Katsumata et al.*, 2003; *Miller et al.*, 2004, 2005], and is illustrated in the slices through the three tomographic models (Figures 2–4). The slab is imaged beneath the Izu arc as subducting at ∼40–45° that bends on top of the 660-km discontinuity (Figure 3, I-I′). Beneath the Kurile arc the subducting slab is dipping at ∼50° and the seismicity falls within the high-velocity zone (Figure 3, K-K′). Beneath the Japan arc the Pacific slab is well defined with an approximate dip of 30° that gradually transitions into a horizontal structure along the 660-km discontinuity (Figure 3, J-J′). The slab that is lying on the 660-km discontinuity appears to be thicker than the slab beneath the Kurile arc that is penetrating through the transition zone at a steeper angle. In Figure 4 the *P* wave tomographic model is presented as a fence diagram that is sliced parallel to the Izu-Japan-Kurile trench location through the forearc and ∼300 km landward from the trench. Figure 4 illustrates the distorted shape of the subducting Pacific plate along the arc, increase in slab thickness from north to south, and complex morphology at the Hokkaido corner.

[13] Alternatively, depth slices through the tomographic images show a strong fast velocity boundary that outlines the slab geometry and position at depth (Figure 5). The amplitude and resolution of the fast velocity perturbations allows for a clear definition of the position of the edge of the subducted Pacific plate. The sharp anomaly boundary at shallow depths is very similar to the current Pacific plate boundary and is measured as distances D_1 and D_2 to the edge of the high-velocity zone at 220 and 520 km depth in the shear wave speed images for the Izu, Japan, and Kurile arcs (Figure 5). The Ryukyu arc that is currently subducting the Philippine Sea plate northwestward beneath the Amurian or Eurasian plate only has a coherent slab down to220 km. However the paleo-Izu-Japan-Kurile arc is clearly defined to 520 km depth.

4. Three-Dimensional Morphology

[14] The complex morphology of the subducting Pacific plate beneath northeast Asia is imaged with a combination

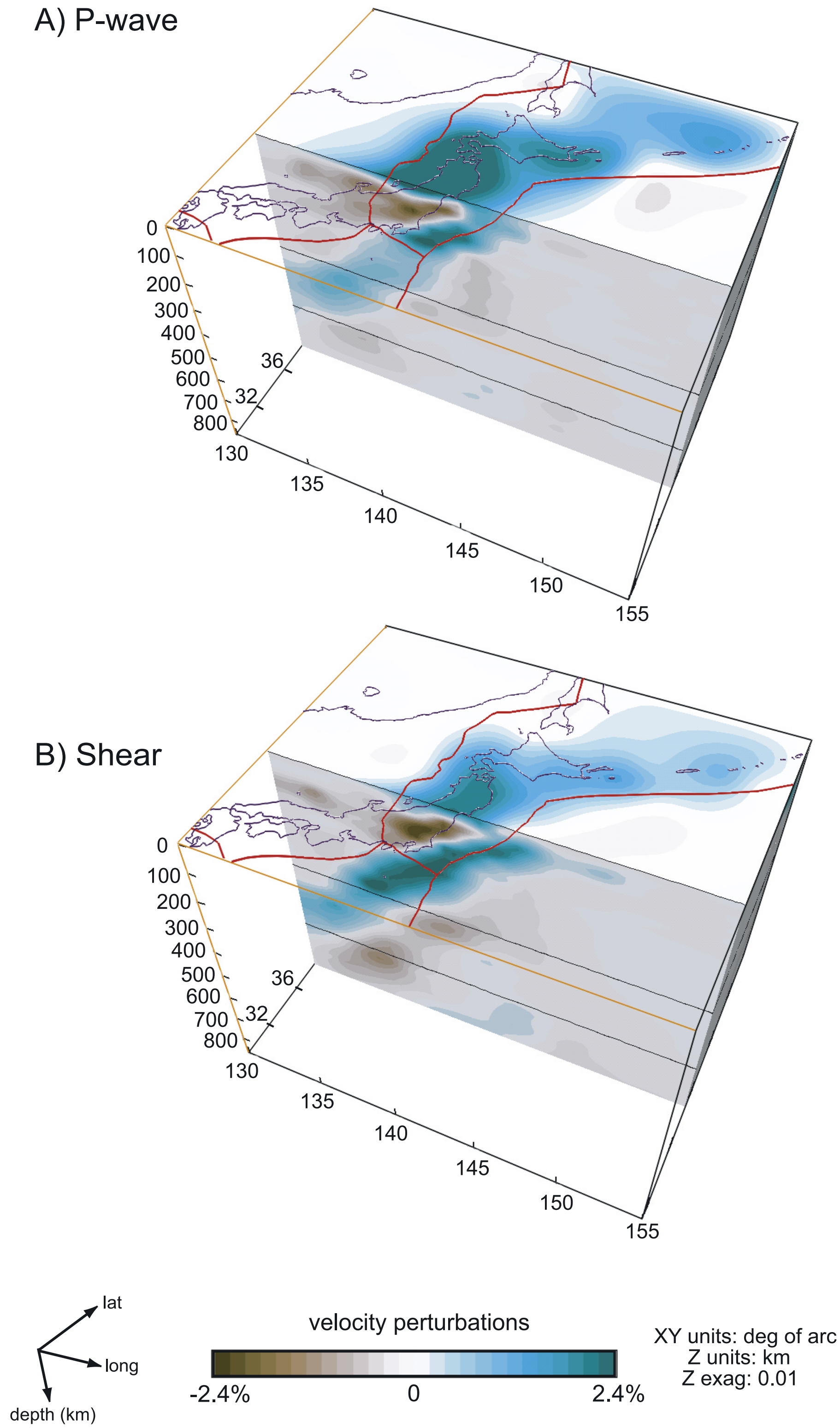

Figure 2. (a) *P* wave and (b) shear wave speed tomographic models of the northwest Pacific region with brown representing the slow velocities and cyan representing the fast velocities in percentage from the reference model ak135 [*Kennett et al.*, 1995]. The models are sliced along 38.5°N latitude (and 5 km depth) with the Asian coastline in purple and the plate boundaries in red, while the two horizontal lines represent the 410- and 660-km discontinuities.

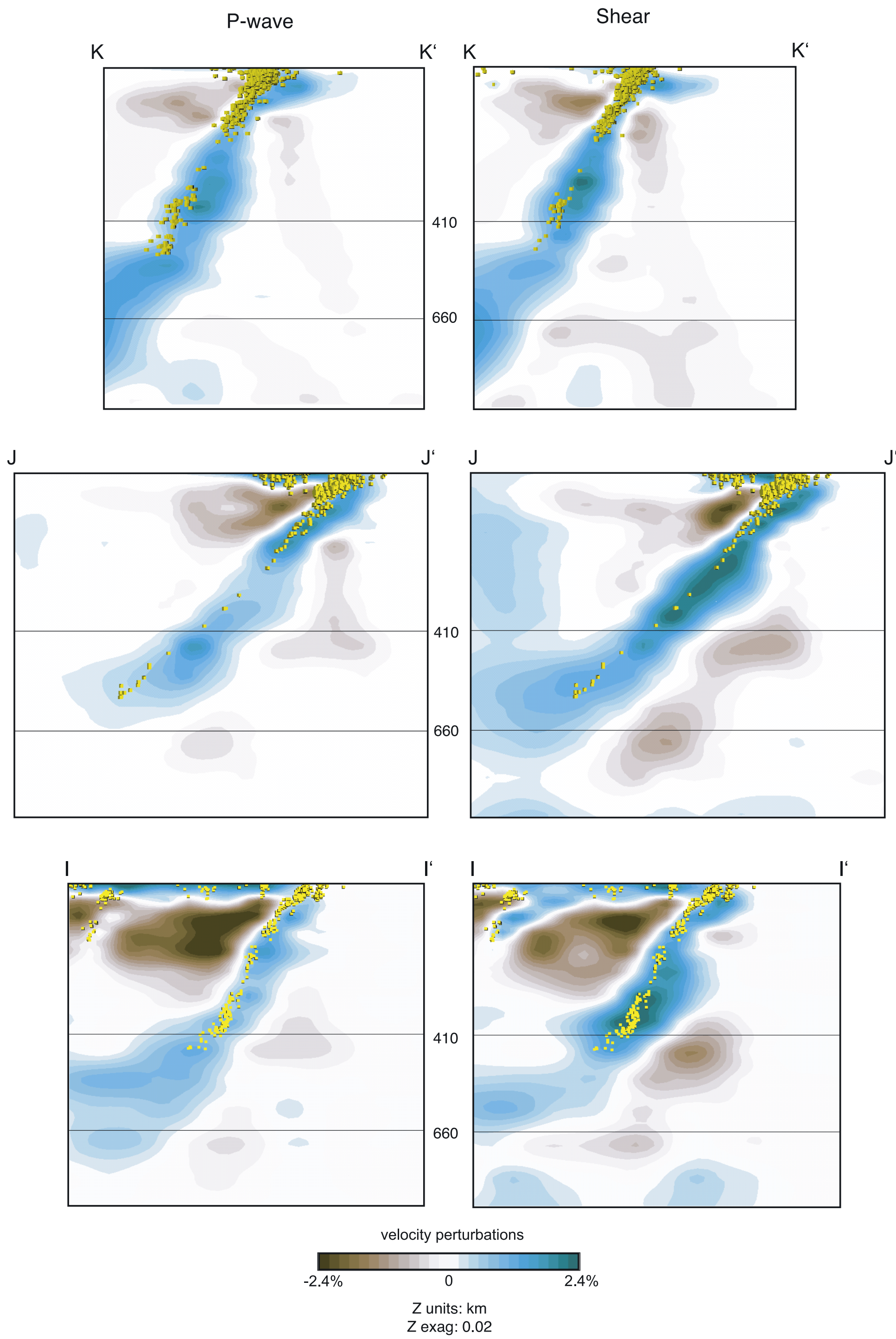

Figure 3. Cross sections through the tomography models (*P* wave and shear wave speed) along locations shown in Figure 1 with hypocenters of events during 1967–1998 with magnitude greater than 4.5 [*Engdahl et al.*, 1998]. Cross sections K-K′ illustrate the steeply dipping Pacific plate beneath the Kurile arc and J-J′ and I-I′ depict the more shallow dipping slab beneath the Japan and Izu arcs.

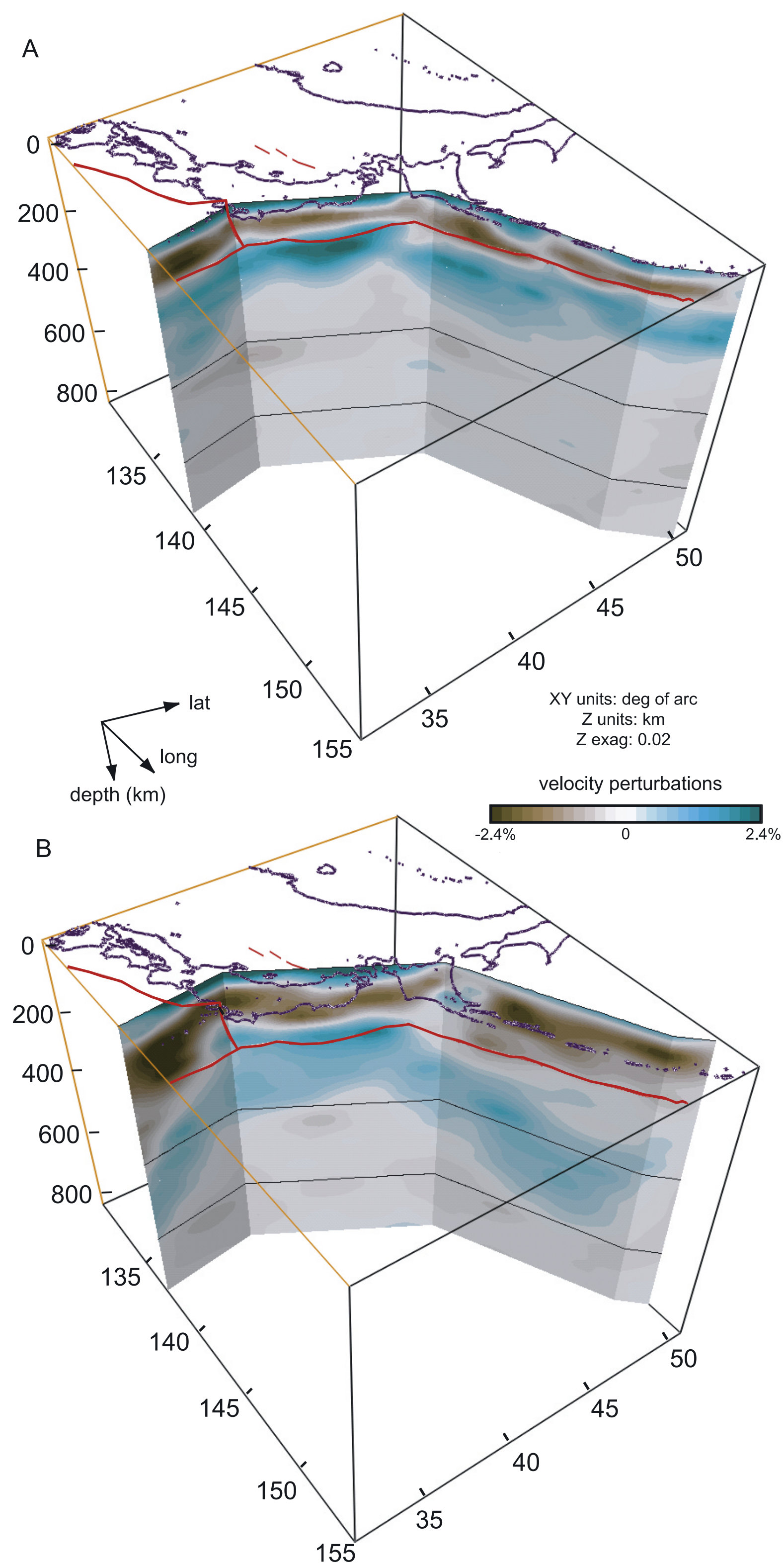

Figure 4. Fence style diagram sliced through the *P* wave tomographic image parallel to the Izu-Japan-Kurile trench approximately through (a) the active volcanic arc and (b) 300 km west of the arc with the Asian coastline drawn in purple and trench in red.

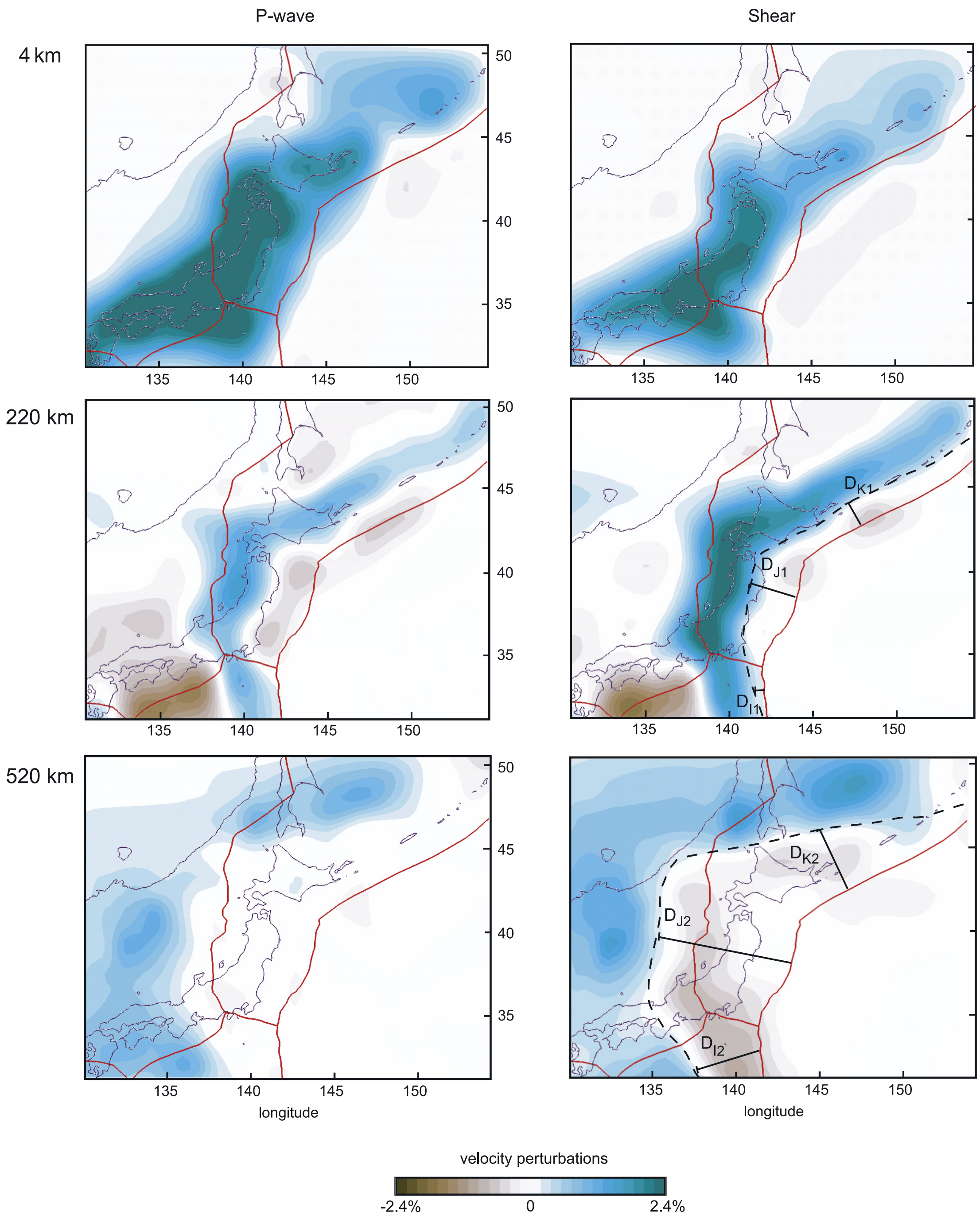

Figure 5. Layer anomaly maps at 4, 220, and 520 km depth for *P* wave and shear wave speed inversions with the Asian coastline in purple and plate boundaries in red for reference. Cyan represents fast velocities and brown represents slow velocities, scaled in percent relative to reference model ak135 [*Kennett et al.*, 1995]. Distances from the current plate boundaries for the Kurile, Japan, and Izu arcs (D_{K1}, D_{K2}, D_{J1}, D_{J2}, D_{I1}, D_{I2}) used in Figures 7 and 8 are shown.

of seismicity and seismic tomography. The tomographic images and shape of the Wadati-Benioff zone (Figures 2–5) were used to construct a three-dimensional interpreted model of the slab geometry. The extent and geometry of the subducting slab was defined by picking the maximum gradient of velocity in the *P* wave model, which compensates for the lower resolution in the northern portion of the model where there are fewer seismic stations. Then the points that were interpreted as the top and bottom of the subducting oceanic lithosphere (~600 points for the top of

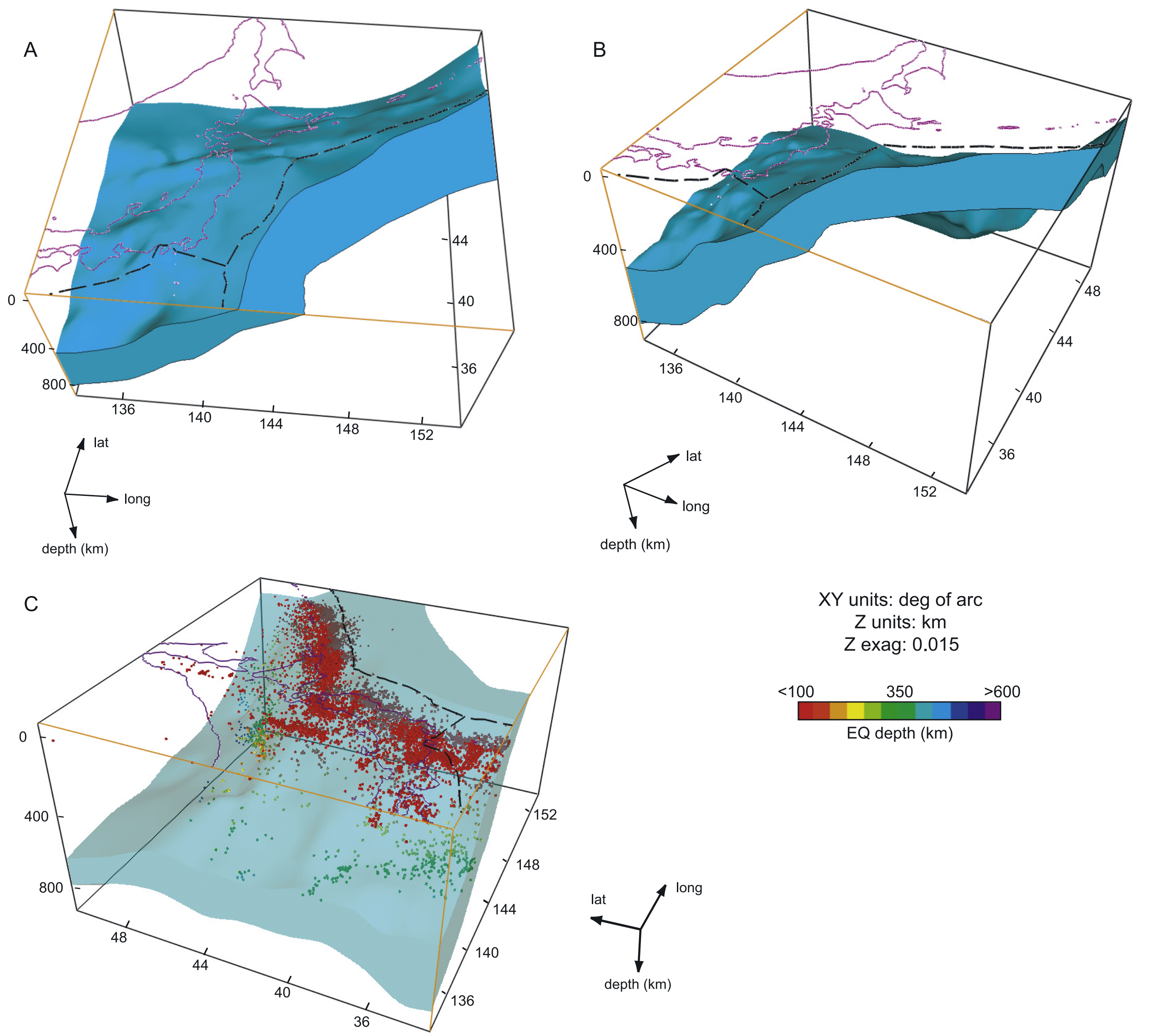

Figure 6. (a–c) Interpreted three-dimensional model of the morphology and geometry of the subducting Pacific plate along the northwest Pacific margin. The Japanese coastline is in purple, current plate boundaries are in black dashed lines, and earthquake events from the *Engdahl et al.* [1998] catalog are color coded with depth in Figure 6c.

the slab and 500 for the bottom of the slab) in the tomographic images were gridded in earthVision© (with grid and interpreted point spacing equaling ~0.25°) to create two surfaces representing the top and bottom of the subducting slab. Then the surfaces were used to create a solid schematic model of the subducting Pacific plate beneath the Kurile and Japan arcs (Figures 6a–6c). The intricate and varying morphology along the arc is then more easily visualized in three dimensions. The change in dip of the slab shown in the cross sections and depth slices through the tomographic images beneath the Izu, Japan, and Kurile arcs is illustrated in the model. The interplate seismicity is shown in Figure 6c when the slab is viewed as transparent to confirm the shape of the subducting Pacific plate is similar to the Wadati-Benioff zone geometry.

[15] The three-dimensional visual model created with earthVision™ software agrees with previous work that the subducting Pacific plate dips between 40° and 50° beneath the Kurile arc, ~30° beneath the Japan arc, and ~45° beneath the Izu arc, and appears to be continuous with a gentle transition at the arc-arc junction of the Hokkaido corner [*Chiu et al.*, 1991; *van der Hilst et al.*, 1991; *Fukao et al.*, 1992; *van der Hilst et al.*, 1993; *Miyamachi et al.*, 1994; *Zhao et al.*, 1997; *Gudmundsson and Sambridge*, 1998; *Gorbatov et al.*, 2000; *Gorbatov and Kennett*, 2003]. The model of the Pacific slab and the tomographic images

both show the slab beneath the Sea of Japan changes dip at the 660-km discontinuity, where it becomes horizontal and gradually widens within the transition zone. Farther south beneath the Izu arc, the slab has a similar geometry to the Japan slab where it also lies horizontally in the transition zone. In contrast, the subducted slab beneath the Kurile arc appears thinner and penetrates into the lower mantle, with only a minor change of dip as it crosses through the transition zone (Figures 3 and 6).

5. Paleogeographic Reconstruction

[16] A new paleogeographic model of the northwest Pacific region was modeled using PlatyPlusPlus software based on previously defined Euler poles for the Pacific, Philippine, Okhotsk, Amurian, and North American plate motions relative to Eurasia. The plate motion data was collected from a series of journal articles [*Seno and Maruyama*, 1984; *Engebretson et al.*, 1985; *Lawver et al.*, 1990; *Seno et al.*, 1993; *Hall et al.*, 1995b; *Seno et al.*, 1996; *Wei and Seno*, 1998; *Zang et al.*, 2002]. Euler poles defined for the more recently defined plates [*Seno et al.*, 1996; *Wei and Seno*, 1998], and new Euler poles [*Zang et al.*, 2002] for the Philippine Sea plate, were incorporated into a more updated data set with the more recently defined boundaries for the Amurian, Okhotsk, Philippine, North American, Pacific and Eurasian plates [*Bird*, 2003]. The Euler pole data were used in PlatyPlusPlus software to reconstruct the position of the plates back to the late Miocene. Table 1 lists the angular velocities for the western Pacific margin reconstruction shown in Figure 7. The interpreted motions of the plates in northwest Pacific are consistent with recent tectonics, geologic data, and interpreted slab morphology from tomographic images. The reconstruction illustrates the Pacific plate converging obliquely along the Kurile arc and orthogonal along the Japan arc, opening of the Kurile basin 8–12 Ma, development of arcuate shape of the Japanese islands as the Sea of Japan opened in the mid-Miocene, right-lateral transpressional motion from Sakhalin south to Hokkaido and NE Honshu, asymmetric motion of the Izu arc, and the collision of the Kurile and Japan arcs (Figure 7).

[17] The Pacific plate has been moving at its current angular velocity around a Euler pole located at 62.33°N, −85.03°E [*Wei and Seno*, 1998] for the past 10 Myr, but has a slightly different pole for the periods of 10–20 Ma and 20–37 Ma [*Engebretson et al.*, 1985]. The fast perpendicular convergence of the Pacific along the Japan arc and oblique convergence along the Kurile arc are illustrated in Figure 7. The Japan arc appears to have been retreating oceanward since the early Miocene and the Kurile arc has been retreating asymmetrically from the early Miocene to ~8 Ma [*Fournier et al.*, 1994; *Jolivet et al.*, 1994; *Schellart et al.*, 2003]. The asymmetrical motion of the Kurile arc appears to be due to the anticlockwise rollback of the subducting Pacific plate, in which the retreat velocity of the hinge line in the southwest is faster when compared to the northeast, while pinned at the cusp at the Aleutian arc junction [*Schellart et al.*, 2003]. After 8 Ma the trench continued to retreat, but extremely slowly. As the Kurile arc retreated, the Kurile basin opened, and similarly, the Sea of Japan has also opened but with a much more complicated motion.

[18] The Izu arc has retreated oceanward from 20 Ma to ~8 Ma when it then reversed direction and advanced [*Miller et al.*, 2006b]. This asymmetric retreat caused the plate boundary to evolve into a more north-south orientation, as opposed to the north-northwest strike that existed in the past. This asymmetric retreat is consistent with the clockwise motion described by other authors in the development of the current Philippine Sea plate [*Seno and Maruyama*, 1984; *Seno et al.*, 1993; *Hall et al.*, 1995a; *Hall*, 2002].

[19] Another important event in the northwest Pacific tectonic history is the initiation of the collision of the Japan and Kurile arcs at the Hokkaido corner at ~11 Ma. This appears to have occurred as a result of the oblique convergence of the Pacific plate and the asymmetric retreat of the Kurile arc. The Japan arc is shown to be retreating eastward since the mid-Miocene at a rate much more rapid than along the Kurile arc. The reconstruction also illustrates the slow southwestward motion of the Okhotsk plate causing some recent shearing (0–6 Ma) in Sahkalin and Hokkaido, although the Euler pole published by *Wei and Seno* [1998] does not accurately describe the transpressional motion that is described in previous studies [*Fournier et al.*, 1994; *Jolivet et al.*, 1994] for ages earlier than the Pliocene. Our model also does not illustrate the amount of shear motion in SW Japan and the region near Korea that is expected by the models described by *Jolivet and Tamaki* [1992] and *Jolivet et al.* [1994] using the Amurian plate rotation poles from *Wei and Seno* [1998].

[20] The Japanese islands are shown to become more arcuate in shape during the past 25 Myr, which is also supported by earlier studies [*Otofuji and Matsuda*, 1984; *Otofuji et al.*, 1985a; *Celaya and McCabe*, 1987; *Otofuji and Matsuda*, 1987; *Hibbard and Karig*, 1990; *Fournier et al.*, 1994; *Jolivet et al.*, 1994]. The Sea of Japan appears have been opening since the early Miocene and the more rapid retreat of central Honshu with the asymmetric retreat of the Kurile arc allows the bending of the Japanese islands to emerge (Figure 7).

6. Discussion

[21] Previous authors have suggested that differing slab geometry can be attributed to the past plate motion history and each subduction zone can be described by different stages of development in the evolutionary process using tomography, geochemistry, and modeling techniques [*Kincaid and Olson*, 1987; *Ringwood and Irifune*, 1988; *van der Hilst and Seno*, 1993; *Griffiths et al.*, 1995; *Schellart et al.*, 2003; *Replumaz et al.*, 2004]. Our new detailed reconstruction of the northwest Pacific and complementing tomographic images can be integrated and compared to understand the tectonic evolution of the past 20 Myr. The combination of tomography models can be used to validate or constrain the estimated location of paleoplate boundaries of the Izu, Japan

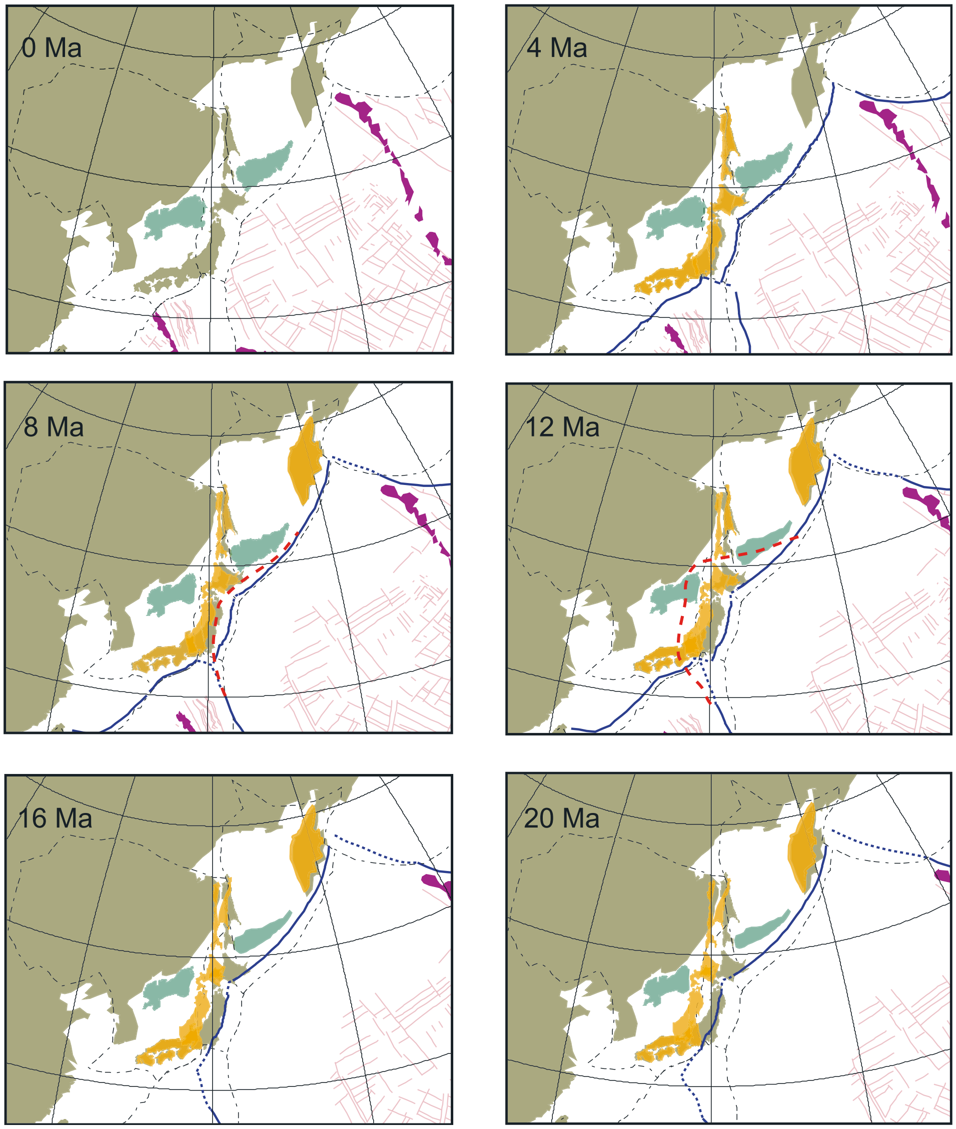

Figure 7. Paleogeographic reconstruction of the northwest Pacific from the mid-Miocene based on new slip vector based Euler poles in Table 1 with plates defined by *Bird* [2003] in fixed black dashed lines. Current coastlines are grey, paleogeographic coastlines are orange, pink lines are magnetic anomalies, blue lines are interpreted paleoplate boundaries with dashed portions for the inferred extensions, green objects are basins, and purple objects are oceanic plateaus or aseismic ridges. The thick red dashed lines are the interpreted paleoboundaries from Figure 5 for depths of 220 and 520 km, which represent the maximum extend of plausible rollback of the Pacific plate for these ages. Note that the Ryukyu arc is not shown for 16 and 20 Ma because we have no evidence of a subducted slab corresponding to that age/depth.

and Kurile arcs assuming similar convergence rates and subduction angles to the present.

[22] In the regional tomographic images the slab beneath the Sea of Japan has a near horizontal orientation and does not extent into the lower mantle (Figures 2–3). The slab beneath the Japan and Izu arcs appear to be stagnant on top of the 660-km discontinuity, which acts as a partial barrier to mature (cold) oceanic lithosphere penetration, and could remain in this position until eventually sinking into the lower mantle after enough mass accumulates [*Ringwood and Irifune*, 1988; *Fukao et al.*, 1992, 2001]. Farther north, the slab beneath the Sea of Okhotsk has partially pierced through the transition zone at a ~50° angle. The slab also appears to be thinner, yet penetrate deeper (below 660 km) below the Kurile arc (Figures 3a–3c), in comparison to the thicker slab beneath the Japan arc that lies on top of the 660-km discontinuity (Figures 3d–3e). The thinner geometry beneath the Kurile arc could be due to the slower, oblique convergence rate (8.2 cm/yr) of the Pacific plate (Figure 1) and a slower trench retreat rate (Figure 7). As the

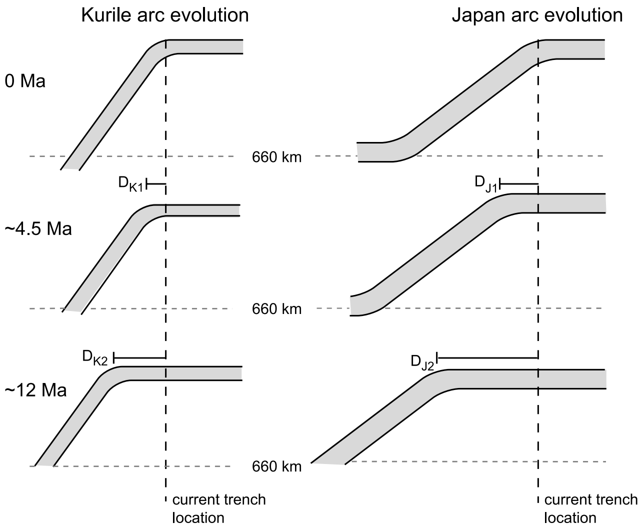

Figure 8. Schematic drawing of the evolution of the slab morphology beneath the Japan and Kurile arcs since the mid-Miocene with estimated ages and approximate distances (D_1, D_2) from current trench position determined from Figure 5 and convergence rates [*DeMets et al.*, 1994]. Beneath Kurile arc, the trench retreats slowly the slab dip remains steep and the subducted oceanic lithosphere penetrates into the lower mantle. Beneath Japan arc, the trench quickly retreats the gentle angle of dip is maintained and the slab in lain down on the 660-km discontinuity.

slab is subducting more slowly it may have had time to accumulate in the mantle transition zone and therefore have enough mass and density to partially penetrate into the lower mantle. As it sinks into the lower mantle it pulls the slab in the upper mantle down, which causes the thinner form. In contrast, the Pacific plate is converging more quickly and perpendicular at the Japan arc causing the slab to spread on top of the 660-km discontinuity. Then as the Japan arc retreated (more quickly than the Kurile arc), the slab did not have enough time for critical amount of subducted mass to accrue, but has thickened as it bent horizontally in the transition zone (Figure 3). The different evolution of the subducting oceanic lithosphere beneath the Kurile and Japan arcs are schematically represented in Figure 8 and illustrating the distance (and rate) of trench retreat for each arc based on the distances estimated in Figure 5.

[23] An important aspect of tectonic history illustrated in the new reconstruction is the collision of the Kurile and Japan arcs at the Hokkaido corner at ~11 Ma (Figure 7). The continuous southwest collision of the Kurile arc into the NE Japan arc has resulted in the Hidaka mountain range. The arc-arc collision appears to be essentially continuous for the past ~11 Myr and therefore expressions of this long-term event should be evident in both the crust and the mantle. Previous studies described the Hidaka mountains as a mid-Miocene age north-northwest trending belt that formed from the arc-arc collision. Further work has investigated the complex velocity structure beneath the Hokkaido corner in terms of the crustal and upper mantle anomalies [*Miyamachi and Moriya*, 1984; *Moriya*, 1986; *Miyamachi and Moriya*, 1987; *Kimura*, 1996; *Moriya et al.*, 1998]. The timing of the collision in our model is consistent with the previous models, and has constrained the collision initiation with additional data confirming of the termination of volcanism in the Hidaka mountains [*Maeda*, 1990; *Maeda and Kagami*, 1996]. The deeper complex structure of the slab beneath the Hokkaido corner has been investigated further by *Miller et al.* [2006a], but here we investigate the regional tectonic history to understand the evolution of the current morphology in a broader context.

[24] Since it appears that the slab thickens beneath the Japan arc in the tomographic images (Figures 2–4), we suggest the continuous southwestward collision of the Kurile arc may cause this atypical (thickened) geometry. The thickened slab beneath northeast Japan may be produced not only by the bending on to the 660-km discontinuity, but also by the accumulation or accretion of subducted oceanic lithosphere as the Kurile arc continuously converges with the Japan arc beneath the Hokkaido corner. Arc-arc collisions have been suggested to be an essential component of continental growth by accumulation [*Tsumura et al.*, 1999], then it reasonable that the deeper structure may become thickened as the two slabs merge at the Hokkaido corner.

[25] The paleogeographic reconstruction in Figure 7 illustrates one possible evolution of the plate boundaries, but it can be interpreted as a conservative model using present-day plate motions and interpreted Euler poles for the past. As an alternative and test of the plausibility of the reconstruction the layer anomaly maps of *P* wave and shear wave speed in Figure 5 were used to estimate the paleoposition of the Pacific plate boundary back in time. The first set of images shows the tomography models sliced at 4 km depth to illustrate the current near surface slab morphology and plate boundary. The next two sets of images are sliced through the upper mantle at 220 and 520 km depth. At 220 km the approximate age of the slab is calculated to be 5.2 Ma at the Izu arc, 4.8 My at the Japan arc, and 4 My at the Kurile arc based on the average convergence rates along the plate boundary [*DeMets et al.*, 1994] and the approximate 45°, 30° and 50° respective dipping angles of subduction. At 520 km depth the age of the slab is estimated to be 12.2, 11.3, and 9.5 Ma, based on the same averaged velocity and slab dip assumptions for the Izu, Japan, and Kurile arcs (Figure 5). From Figure 5 it appears that 4–5 Ma the plate boundary had a similar shape to the current Japan-Kurile arc and the Izu arc had a trend slightly more northwesterly than its current near N-S strike. At 520 km depth the Kurile arc appears to be striking west-southwest, which illustrates that that the slab has rolled back asymmetrically ~500 km (D_{K2}). The Japan arc in the 520 km depth slice has approximately the same strike as its present configuration but has migrated a considerable father distance than the Kurile arc (D_{J2} is ~850 km). From these approximations and images it can be confirmed that the Japan arc has migrated eastward at a rate more rapid that the asymmetrical migration of the Kurile arc as seen in the paleogeographic reconstructions (Figure 7). It is also evident that the Izu arc

has also retreated asymmetrically as it had more northwestward trend between 8 and 20 Ma (Figure 5), which describes the entire northwest Pacific convergent margin (Izu-Japan-Kurile arc system) becoming less convex through time in both of the plate configuration models.

[26] The Euler poles that describe the motion of the plates in the western Pacific (Table 1) provide a more accurate model than previous reconstructions, which neglect the Amurian and Okhotsk plates [*Seno and Maruyama*, 1984; *Otsuki*, 1990; *Jolivet et al.*, 1994; *Hall et al.*, 1995a; *Hall*, 2002]. However, the new reconstruction still does not completely explain the subducted slab geometry seen in the tomographic images (Figure 7). One of the factors that may be attributed to the misfit is the assumption that the plates are rigid during the timescale of the model. As evident in the subducted slab morphology in the three-dimensional models (Figure 7), the plates do not behave rigidly at depth during this 20 Myr time frame; therefore it is very likely that they do not behave rigidly at the surface of the Earth. However, this assumption was made in order to compare the new reconstruction to the previous models [*Seno and Maruyama*, 1984; *Otsuki*, 1990; *Jolivet et al.*, 1994; *Hall et al.*, 1995a; *Hall*, 2002].

[27] Another factor that may contribute to the discrepancies in the interpreted past plate boundaries is the assumption that the dip along each of the arcs has remained relatively constant. To assess the error associated with this assumption, a change of up to 10° from the tomographically imaged dips was calculated for each of the Kurile (40°), Japan (30°), and Izu-Bonin (50°) arcs. This did not effect the age of the slab by more than ~15%, which represents only a small difference in age and interpreted position of the plate boundary. Therefore this assumption may have a small impact on the differences between the two tectonic reconstructions, but is not a major contributing factor.

[28] The evolution of curvature of the Japanese Islands has been a continuous subject of research. As previously mentioned, one group of researchers have used paleomagnetic data to describe how the islands underwent a "swinging-door" type motion to develop into their current form [*Otofuji and Matsuda*, 1983; *Otofuji et al.*, 1985b; *Otofuji and Matsuda*, 1987], and another group describe the evolution in terms of shear zones [*Jolivet et al.*, 1991; *Jolivet and Tamaki*, 1992; *Fournier et al.*, 1994]. We propose bending of the Japanese Island Arc is due to the rapid rate of trench retreat along the Japan arc and the asymmetric hinge motion of the Kurile and Izu arcs. In Figures 5 and 7 it can be seen that the Japanese islands could have trended north-south along the paleoplate boundary at ~15 Ma if trench retreat and plate motions have been relatively consistent since the mid-Miocene. This deduction generally agrees with the paleomagnetic data previously published and the tomography images that describe the past position and orientation of the plate boundaries, but describes a more recent and rapid opening of the Sea of Japan. The interpretation of the paleoplate boundaries from the tomographic images can provide a maximum limit to the extent of rollback of the slab (or trench retreat) and the paleogeographic reconstruction based on Euler pole motions can be used a minimum limit.

7. Conclusions

[29] Plate motions and subducting slab morphology are intricately connected and through the integration of modeling seismicity, tomographic images, and relative plate motions the evolution of mantle structure can be unraveled. We have found that the subducted Pacific plate beneath the Japan and Kurile arcs is coherent, but is very complex at the junction of the two arcs near the Hokkaido corner, as the slab subduction angle decreases from north to south while the slab thickens. The stagnant slab beneath the Japan arc appears to be due to a less steep subduction angle, perpendicular convergence of the Pacific plate, and a rapid trench retreat as seen in the new reconstruction and tomographic images. In contrast, the slab beneath the Kurile arc is subducting at a steeper angle and is penetrating through the transition zone and into the lower mantle. This appears to be caused by the slower, oblique convergence of the Pacific plate and slower trench retreat since the opening of the Kurile Basin. The combination of the two asymmetrical trench retreats of the Izu and Kurile arcs with the rapid slab rollback of the Japan arc has resulted in the northwestern Pacific margin to become less arcuate in shape during the Cenozoic.

[30] **Acknowledgments.** We would like to thank Alexei Gorbatov (Geoscience Australia) for the use of tomographic models and Virginia Toy (University of Otago) for discussions about plate tectonics. We also wish to thank one anonymous reviewer, S. Rost, K. Stuewe, O. Oncken, and C. Noll for comments and suggestions that greatly improved the manuscript.

References

Bird, P. (2003), An updated digital model of plate boundaries, *Geochem. Geophys. Geosyst.*, *4*(3), 1027, doi:10.1029/2001GC000252.

Burbach, G. V., and C. Frohlich (1986), Intermediate and deep seismicity and lateral structure of subducted lithosphere in the Circum-Pacific region, *Res. Geophys.*, *24*, 833–874.

Celaya, M., and R. McCabe (1987), Kinematic model for the opening of the Sea of Japan and the bending of the Japanese islands, *Geology*, *15*, 53–57.

Chiu, J.-M., B. L. Isacks, and R. K. Cardwell (1991), 3-D configuration of subducted lithosphere in the western Pacific, *Geophys. J. Int.*, *106*, 99–112.

DeMets, C., R. G. Gordon, D. D. Argus, and S. Stein (1994), Effect of recent revisions to the geomagnetic reversal time scale on estimates of current plate motions, *Geophys. Res. Lett.*, *21*, 2191–2194.

Engdahl, E. R., R. D. van der Hilst, and R. Buland (1998), Global teleseismic earthquake relocation with improved travel times and procedures for depth determination, *Bull. Seismol. Soc. Am.*, *88*, 722–743.

Engebretson, D. C., A. Cox, and R. G. Gordon (1985), Relative motions between oceanic and continental plates in the Pacific Basin, *Spec. Pap. Geol. Soc. Am.*, *206*, 59 pp.

Fournier, M., L. Jolivet, P. Huchon, K. F. Sergeyev, and L. S. Oscorbin (1994), Neogene strike-slip faulting in Sakhalin and the Japan Sea opening, *J. Geophys. Res.*, *99*, 2701–2726.

Fukao, Y., M. Obayashi, H. Inoue, and M. Nenbai (1992), Subducting slabs stagnant in the mantle transition zone, *J. Geophys. Res.*, *97*, 4809–4822.

Fukao, Y., S. Widiyantoro, and M. Obayashi (2001), Stagnant slabs in the upper and lower mantle transition region, *Res. Geophys.*, *39*, 291–323.

Gorbatov, A., and B. L. N. Kennett (2003), Joint bulk-sound and shear tomography for western Pacific subduction zones, *Earth Planet. Sci. Lett.*, *210*, 527–543.

Gorbatov, A., J. Dominguez, G. Suarez, V. Kostoglodov, and D. Zhao (1999), Tomographic images of the *P*-wave velocity structure beneath the Kamchatka peninsula, *Geophys. J. Int.*, *137*, 269–279.

Gorbatov, A., S. Widiyantoro, Y. Fukao, and E. Gordeev (2000), Signature of remnant slabs in the North Pacific from P-wave tomography, *Geophys. J. Int.*, *142*, 27–36.

Griffiths, R. W., R. I. Hackney, and R. D. van der Hilst (1995), A laboratory investigation of effects of trench migration on the descent of subducted slabs, *Earth Planet. Sci. Lett.*, *133*, 1–17.

Gudmundsson, O., and M. Sambridge (1998), A regionalized upper mantle seismic model, *J. Geophys. Res.*, *103*, 7121–7136.

Hall, R. (2002), Cenozoic geological and plate tectonic evolution of SE Asia and the SW Pacific: Computer-based reconstructions, model and animations, *J. Asian Earth Sci.*, *20*, 353–431.

Hall, R., J. R. Ali, C. D. Anderson, and S. J. Baker (1995a), Origin and motion history of the Philippine Sea plate, *Tectonophysics*, *251*, 229–250.

Hall, R., M. Fuller, J. R. Ali, and C. D. Anderson (1995b), The Philippine Sea plate: Magnetism and Reconstructions, in *Active Margins and Marginal Basins of the Western Pacific*, *Geophys. Monogr. Ser.*, vol. 88, edited by B. Taylor and J. Netland, pp. 371–404, AGU, Washington, D. C.

Hibbard, J. P., and D. E. Karig (1990), Alternative plate model for the early Miocene evolution of the southwest Japan margin, *Geology*, *18*, 170–174.

Jolivet, L., and K. Tamaki (1992), Neogene kinematics in the Japan Sea region and the volcanic activity of the northeast Japan arc, *Proc. Ocean Drill. Program Sci. Results*, *127–128*, 1311–1331.

Jolivet, L., P. Huchon, and C. Rangin (1989), Tectonic setting of western Pacific marginal basins, *Tectonophysics*, *160*, 23–47.

Jolivet, L., P. Huchon, J. P. Brun, N. Chamot-Rooke, X. Le Pichon, and J. C. Thomas (1991), arc deformation and marginal basin opening, Japan Sea as a case study, *J. Geophys. Res.*, *96*, 4367–4384.

Jolivet, L., K. Tamaki, and M. Fournier (1994), Japan Sea, opening history and mechanism; a synthesis, *J. Geophys. Res.*, *99*, 22,237–22,259.

Jolivet, L., C. Faccenna, N. D'Agostino, M. Fournier, and D. M. Worrall (1999), The kinematics of backarc basins, examples from the Tyrrhenian, Aegean and Japan seas, in *Continental Tectonics*, edited by C. MacNiocaill and P. D. Ryan, *Geol. Soc. Spec. Publ.*, *164*, 21–53.

Katsumata, K., N. Wada, and M. Kasahara (2003), Newly imaged shape of the deep seismic zone within the subducting Pacific plate beneath the Hokkaido corner, Japan-Kurile arc-arc junction, *J. Geophys. Res.*, *108*(B12), 2565, doi:10.1029/2002JB002175.

Kennett, B. L. N., and A. Gorbatov (2004), Seismic heterogeneity in the mantle -strong shear wave signature of slabs from joint tomography, *Phys. Earth Planet. Inter.*, *146*, 88–100.

Kennett, B. L. N., E. R. Engdahl, and R. Buland (1995), Constraints on seismic velocities in the Earth from traveltimes, *Geophys. J. Int.*, *122*, 108–124.

Kennett, B. L. N., S. Widiyantoro, and R. D. van der Hilst (1998), Joint seismic tomography for bulk sound and shear wave speed in the Earth's mantle, *J. Geophys. Res.*, *103*, 12,469–12,493.

Kimura, G. (1996), Collision orogeny of arc-arc junctions in the Japanese Islands, *Island Arc*, *5*, 262–275.

Kincaid, C., and P. Olson (1987), An experimental study of subduction and slab migration, *J. Geophys. Res.*, *92*, 13,832–13,840.

Lawver, L. A., R. D. Muller, S. P. Srivastava, and W. R. Roest (1990), The opening of the Arctic Ocean, in *Geologic History of the Polar Oceans: Arctic Versus Antarctic*, *NATO Sci. Ser. C*, vol. 308, edited by U. Bleil and J. Thiede, pp. 29–62, Springer, New York.

Maeda, J. (1990), Opening of the Kuril Basin deduced from the magmatic history of central Hokkaido, north Japan, *Tectonophysics*, *174*, 235–255.

Maeda, J., and H. Kagami (1996), Interaction of a spreading ridge and an accretionary prism: Implications from MORB magmatism in the Hidaka magmatic zone, Hokkaido, Japan, *Geology*, *24*, 31–34.

Miller, M. S., B. L. N. Kennett, and G. S. Lister (2004), Imaging changes in morphology, geometry, and physical properties of the subducting Pacific plate along the Izu-Bonin-Mariana arc, *Earth Planet. Sci. Lett.*, *224*, 363–370.

Miller, M. S., A. Gorbatov, and B. L. N. Kennett (2005), Heterogeneity within the subducting Pacific slab beneath the Izu-Bonin-Mariana arc: Evidence from tomography using 3D ray-tracing inversion techniques, *Earth Planet. Sci. Lett.*, *235*, 331–342.

Miller, M. S., B. L. N. Kennett, and A. Gorbatov (2006a), Morphology of the distorted subducted Pacific slab beneath the Hokkaido corner, Japan, *Phys. Earth Planet. Inter.*, *156*, 1–11.

Miller, M. S., B. L. N. Kennett, and V. G. Toy (2006b), Spatial and temporal evolution of the subducting Pacific plate structure along the western Pacific margin, *J. Geophys. Res.*, *111*, B02401, doi:10.1029/2005JB003705.

Miyamachi, H., and T. Moriya (1984), Velocity structure beneath the Hidaka Mountains in Hokkaido, Japan, *J. Phys. Earth*, *32*, 13–42.

Miyamachi, H., and T. Moriya (1987), Velocity structure and aftershock distribution of the Urakawa-oki earthquake, *J. Phys. Earth*, *35*, 309–326.

Miyamachi, H., M. Kasahara, S. Suzuki, K. Tanaka, and A. Hawegawa (1994), Seismic velocity structure in the crust and upper mantle beneath Northern Japan, *J. Phys. Earth*, *42*, 269–301.

Moriya, T. (1986), Collision of forearcs and overlapped deep seismic zone in the transitional zone between the Northern Honshu and Kurile arcs, *J. Phys. Earth*, *34*, S175–S192.

Moriya, T., H. Okada, T. Matsushima, S. Asano, T. Yoshii, and A. Ikami (1998), Collision structure in the upper crust beneath the southwestern foot of the Hidaka Mountains, Hokkaido, Japan as derived from explosion seismic observations, *Tectonophysics*, *290*, 181–196.

Otofuji, Y., and T. Matsuda (1983), Paleomagnetic evidence for the clockwise rotation of southwest Japan, *Earth Planet. Sci. Lett.*, *62*, 349–359.

Otofuji, Y., and T. Matsuda (1984), Timing of rotational motion of southwest Japan inferred from paleomagnetism, *Earth Planet. Sci. Lett.*, *70*, 343–382.

Otofuji, Y., and T. Matsuda (1987), Amount of rotational motion of southwest Japan: Fan shape opening of the southwestern part of the Japan Sea, *Earth Planet. Sci. Lett.*, *85*, 289–301.

Otofuji, Y., T. Matsuda, and S. Nohda (1985a), Paleomagnetic evidence of the Miocene counterclockwise rotation of northeast Japan-rifting process of the Japan arc, *Earth Planet. Sci. Lett.*, *75*, 265–277.

Otofuji, Y., T. Matsuda, and T. Nohda (1985b), Opening mode of the Japan Sea inferred from the paleomagnetism of the Japan arc, *Nature*, *317*, 603–604.

Otsuki, K. (1990), Westward migration of the Izu-Bonin Trench, northward motion of the Philippine Sea plate, and their relationships to the Cenozoic tectonics of Japanese island arcs, *Tectonophysics*, *180*, 351–367.

Replumaz, A., H. Karason, R. D. van der Hilst, J. Besse, and P. Tapponnier (2004), 4-D evolution of SE Asia's mantle from geological reconstructions and seismic tomography, *Earth Planet. Sci. Lett.*, *221*, 103–115.

Ringwood, A. E., and T. Irifune (1988), Nature of the 650 km seismic discontinuity: Implications for mantle dynamics and differentiation, *Nature*, *331*, 131–136.

Schellart, W. P., M. W. Jessell, and G. S. Lister (2003), Asymmetric deformation in the backarc region of the Kuril arc, northwest Pacific: New insights from analogue modeling, *Tectonics*, *22*(5), 1047, doi:10.1029/2002TC001473.

Seno, T., and S. Maruyama (1984), Paleogeographic reconstruction and origin of the Philippine Sea, *Tectonophysics*, *102*, 53–84.

Seno, T., S. Stein, and A. E. Gripp (1993), A model for the motion of the Philippine Sea plate consistent with NUVEL-1 and geological data, *J. Geophys. Res.*, *98*, 17,941–17,948.

Seno, T., T. Sakurai, and S. Stein (1996), Can the Okhotsk plate be discriminated from the North American plate?, *J. Geophys. Res.*, *101*, 11,305–11,315.

Tsumura, N., H. Ikawa, T. Ikawa, M. Shinohara, T. Ito, K. Arita, T. Moriya, G. Kimura, and T. Ikawa (1999), Delamination-wedge structure beneath the Hidaka Collision Zone, Central Hokkaido, Japan inferred from seismic profiling, *Geophys. Res. Lett.*, *26*, 1057–1060.

van der Hilst, R., and T. Seno (1993), Effects of relative plate motion on the deep structure and penetration depth of slabs below the Izu-Bonin and Mariana island arcs, *Earth Planet. Sci. Lett.*, *120*, 395–407.

van der Hilst, R. D., E. R. Engdahl, W. Spakman, and G. Nolet (1991), Tomographic imaging of subducted lithosphere below northwest Pacific island arcs, *Nature*, *353*, 37–43.

van der Hilst, R. D., E. R. Engdahl, and W. Spakman (1993), Tomographic inversion of *P* and *pP* data for aspherical mantle structure below the northwest Pacific region, *Geophys. J. Int.*, *115*, 264–302.

Wei, D., and T. Seno (1998), Determination of the Amurian plate motion, in *Mantle Dynamics and Plate Interactions in East Asia*, *Geodyn. Ser.*, vol. 27, edited by M. F. J. Flower et al., pp. 337–346, AGU, Washington, D. C.

Widiyantoro, S. (1997), Studies of seismic tomography on regional and global scale, Ph.D. thesis, 256 pp., Aust. Natl. Univ., Canberra.

Widiyantoro, S., B. L. N. Kennett, and R. D. van der Hilst (1999), Seismic tomography with P and S data reveals lateral variations in the rigidity of deep slabs, *Earth Planet. Sci. Lett.*, *173*, 91–100.

Widiyantoro, S., A. Gorbatov, B. L. N. Kennett, and Y. Fukao (2000), Improving global shear wave traveltime tomography using three-dimensional ray tracing and iterative inversion, *Geophys. J. Int.*, *141*, 747–758.

Zang, S. X., Q. Y. Chen, J. Y. Ning, Z. K. Shen, and Y. G. Liu (2002), Motion of the Philippine Sea plate consistent with the NUVEL-1A model, *Geophys. J. Int.*, *150*, 809–819.

Zhao, D., and A. Hasegawa (1993), P wave tomographic imaging of the crust and upper mantle beneath the Japan Islands, *J. Geophys. Res.*, *98*, 4333–4353.

Zhao, D., A. Hasegawa, and S. Horiuchi (1992a), Tomographic imaging of *P* and *S* wave velocity structure beneath northeastern Japan, *J. Geophys. Res.*, *97*, 19,909–19,928.

Zhao, D., S. Horiuchi, and A. Hasegawa (1992b), Seismic velocity structure of the crust beneath the Japan Islands, *Tectonophysics*, *212*, 289–301.

Zhao, D., A. Hasegawa, and H. Kanamori (1994), Deep structure of Japan subduction zone as derived from local, regional, and teleseismic events, *J. Geophys. Res.*, *99*, 22,313–22,329.

Zhao, D., T. Matsuzawa, and A. Hasegawa (1997), Morphology of the subducting slab boundary in the northeastern Japan arc, *Phys. Earth Planet. Inter.*, *102*, 89–104.

Zhou, H.-W., D. L. Anderson, and R. W. Clayton (1990), Modeling of residual spheres for subduction zone earthquakes: Apparent slab penetration signatures in the NW Pacific caused by deep diffuse mantle anomalies, *J. Geophys. Res.*, *95*, 6799–6827.

B. L. N. Kennett and M. S. Miller, Research School of Earth Sciences, Australian National University, Mills Road, Building 61, Canberra, ACT 0200, Australia. (meghan.miller@anu.edu.au)